

# Molecular fingerprinting with the resolved modes of a femtosecond laser frequency comb

Scott A. Diddams<sup>1</sup>, Leo Hollberg<sup>1</sup> & Vela Mbele<sup>1,2,3</sup>

The control of the broadband frequency comb<sup>1</sup> emitted from a mode-locked femtosecond laser has permitted a wide range of scientific and technological advances—ranging from the counting of optical cycles for next-generation atomic clocks<sup>1,2</sup> to measurements of phase-sensitive high-field processes<sup>3</sup>. A unique advantage of the stabilized frequency comb is that it provides, in a single laser beam, about a million optical modes with very narrow linewidths<sup>4</sup> and absolute frequency positions known to better than one part in  $10^{15}$  (ref. 5). One important application of this vast array of highly coherent optical fields is precision spectroscopy, in which a large number of modes can be used to map internal atomic energy structure and dynamics<sup>6,7</sup>. However, an efficient means of simultaneously identifying, addressing and measuring the amplitude or relative phase of individual modes has not existed. Here we use a high-resolution disperser<sup>8,9</sup> to separate the individual modes of a stabilized frequency comb into a two-dimensional array in the image plane of the spectrometer. We illustrate the power of this technique for high-resolution spectral fingerprinting of molecular iodine vapour, acquiring in a few milliseconds absorption images covering over 6 THz of bandwidth with high frequency resolution.

Our technique for direct and parallel accessing of stabilized frequency comb modes could find application in high-bandwidth spread-spectrum communications with increased security, high-resolution coherent quantum control, and arbitrary optical waveform synthesis<sup>10</sup> with control at the optical radian level.

The proposition of using the frequency comb from a mode-locked laser for optical spectroscopy has existed for at least three decades. The proposal and early experiments of groups in Novosibirsk and Stanford<sup>11,12</sup> highlighted the advantages of a mode-locked laser frequency comb for two-photon spectroscopy. The more recent developments in stabilization of the carrier-envelope offset frequency<sup>1,13</sup> provide powerful new tools that have led to recent advances in high-resolution ( $\sim 10^{-11}$ ) spectroscopy performed directly with the output of the mode-locked laser<sup>6,7</sup>. In all such experiments, the various atomic systems under study acted as the high-resolution spectral discriminator that effectively selected an individual frequency comb element (or groups of comb elements) out of a greater number of elements that passed through the sample. Here we take a significantly different approach, in which a high-resolution spectrometer is used to spatially separate and resolve individual comb elements in a

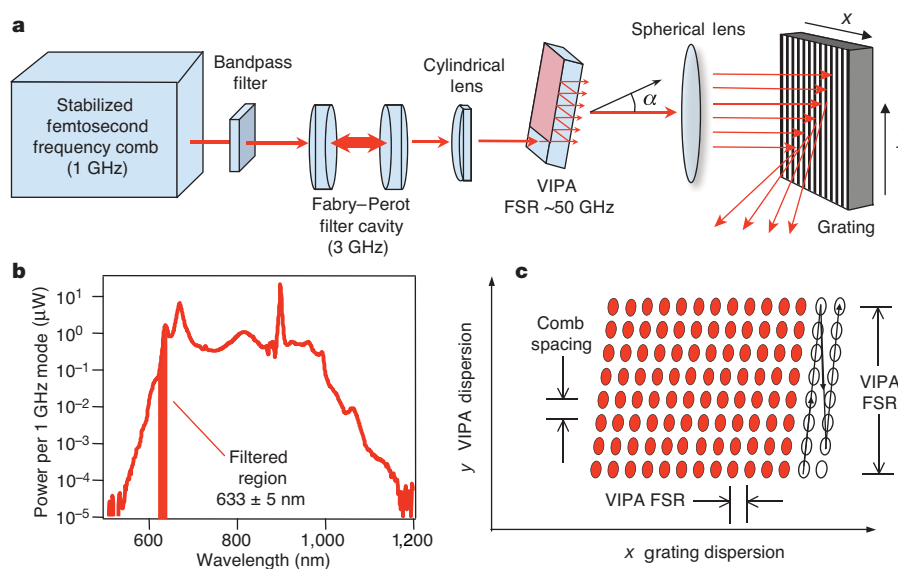


**Figure 1 | Experimental set-up.** **a**, A high-resolution virtually imaged phased array (VIPA) disperser is used in combination with a diffraction grating to spatially resolve the stabilized frequency comb of a Ti:sapphire femtosecond laser. The full output spectrum of the laser and the 633 nm region isolated by the bandpass filter are shown in **b**. The spectrometer output consists of a two-dimensional array of the frequency comb modes, where each 'dot' represents an individual mode (**c**). Within a column ( $y$ ),

which is tilted by the grating dispersion, the dots are separated by the mode spacing (3 GHz in this case). Within each row ( $x$ ), the dots are separated by the VIPA free spectral range (FSR,  $\sim 50$  GHz in this case)<sup>17</sup>. The manner in which successive modes can be indexed and counted is indicated by the arrows in the rightmost two columns. For clarity, not all modes are shown in this diagram.

<sup>1</sup>Time and Frequency Division, National Institute of Standards and Technology, 325 Broadway, Boulder, Colorado 80305, USA. <sup>2</sup>CSIR, NML, PO Box 395, Pretoria, ZA-0001, South Africa. <sup>3</sup>School of Physics, University of the Witwatersrand, Johannesburg, ZA-2050, South Africa.

parallel architecture. Thus, a multi-channel detector can measure the amplitude of the individual comb elements. Using a fraction of the input field as a reference, the relative phase shift introduced by a resonant transition could also be measured with an approach similar to spectral interferometry<sup>14</sup>.

Our approach is shown schematically in Fig. 1a. The frequency comb is produced with a broadband Ti:sapphire laser having a repetition rate  $f_{\text{rep}} = 1$  GHz (refs 15, 16). Both the carrier-envelope offset frequency ( $f_0$ ) and  $f_{\text{rep}}$  are stabilized to a low-noise microwave frequency standard (a hydrogen maser), such that the frequency of each element of the comb may be determined absolutely with a fractional uncertainty at or below  $\sim 2 \times 10^{-13}$  for averaging times of 1 s and longer. Although an optical reference would provide  $\sim 1$  Hz optical resolution<sup>4</sup> and fractional uncertainty into the  $10^{-17}$  range<sup>5</sup>, the microwave reference is sufficient for these experiments. Indeed, for most spectroscopy experiments we could imagine, the atomic reference provided freely by the global positioning system (GPS) would be more than adequate. The output of the Ti:sapphire laser spans roughly 600–1,000 nm, providing tremendous bandwidth for spectroscopic measurements (Fig. 1b). However, imaging and recording the full bandwidth in a single measurement proved challenging. Thus we use an optical bandpass filter to restrict the spectrum to 10 nm of bandwidth around 633 nm, which still provides  $\sim 75$  billion resolvable spectral bins in 1 s of averaging. Within this 10 nm bandwidth, a Fabry–Perot cavity (finesse  $\sim 300$ ) consisting of two spherical mirrors is used to further filter (thin) the frequency comb to a mode spacing of  $3f_{\text{rep}}$ , which better matches the resolution of the spectrometer that follows. By changing the length of the Fabry–Perot cavity, we have filtered the comb at integer multiples of the repetition rate up to  $14f_{\text{rep}}$ . Such flexible filtering of the comb is useful not only in spectroscopy, but also for waveform synthesis and communications applications.

The high-resolution spectrometer (Fig. 1a) provides  $\sim 1.2$  GHz resolution in the visible (633 nm) spectral region by combining a virtually imaged phased array (VIPA) spectral disperser<sup>8</sup> with a conventional grating in an orthogonal arrangement<sup>9,17</sup>. The VIPA is essentially a plane-parallel solid etalon, where the input beam (focused to a line) is injected at an angle through an uncoated

entrance window on the front face. The remainder of the front face is coated with a high-reflective dielectric coating, while the back face has a dielectric coating with 96% reflectivity. The multiple reflections within the VIPA etalon interfere such that the exiting beam has its different frequencies emerging at different angles. As with all etalons, the VIPA has a free spectral range (FSR;  $\sim 50$  GHz in this case) determined by its thickness and material index of refraction. The result is that for an input with spectral bandwidth greater than 50 GHz, the output orders are spatially superimposed on each other. This problem is well known in classical spectroscopy, and has been overcome by using a second dispersive element along an orthogonal spatial dimension<sup>18</sup>. Recent implementations, directed towards separating densely spaced optical communications channels, use a diffraction grating orthogonal to the VIPA<sup>9,17</sup>. In such a case, the grating should provide spectral resolution better than that of the VIPA's FSR. We achieve  $\sim 20$  GHz resolution for visible light with a 2,400 lines  $\text{mm}^{-1}$  grating used at a large angle of incidence, such that  $\sim 24,000$  lines of the grating are illuminated.

The output of the VIPA/grating spectrometer is imaged onto a charge-coupled device (CCD) camera (6.7  $\mu\text{m}$  pixel pitch), resulting in an array of 'dots', representing the power of the individual comb modes spaced by 3 GHz. Thus, the spectrometer transfers the one-dimensional comb into something more reminiscent of a two-dimensional 'brush'. This is illustrated in Fig. 1c, while actual data are shown in Fig. 2a. In the vertical direction of this image, the data repeats every 50 GHz at the FSR of the VIPA, and a subset of unique data are enclosed by the black boxes superimposed on the data of Fig. 2. Inside this boundary, almost 2,200 individual modes can be clearly resolved, spanning the  $\sim 6.5$  THz bandwidth captured on the CCD. The skew of the columns of modes results from the particular choice of the 3 GHz mode spacing, the FSR of the VIPA, the angular dispersion of the grating, and additionally, a slight rotation of the experimental apparatus relative to the camera axes. The repetitive nature of the data in the vertical direction is more evident in Fig. 2b, which is an image acquired in 5 ms with an iodine vapour cell inserted in the beam path before the spectrometer. The cell is at room temperature (25 °C), and multi-passed to yield an equivalent length of  $\sim 2$  m. As seen, numerous modes are attenuated owing to their

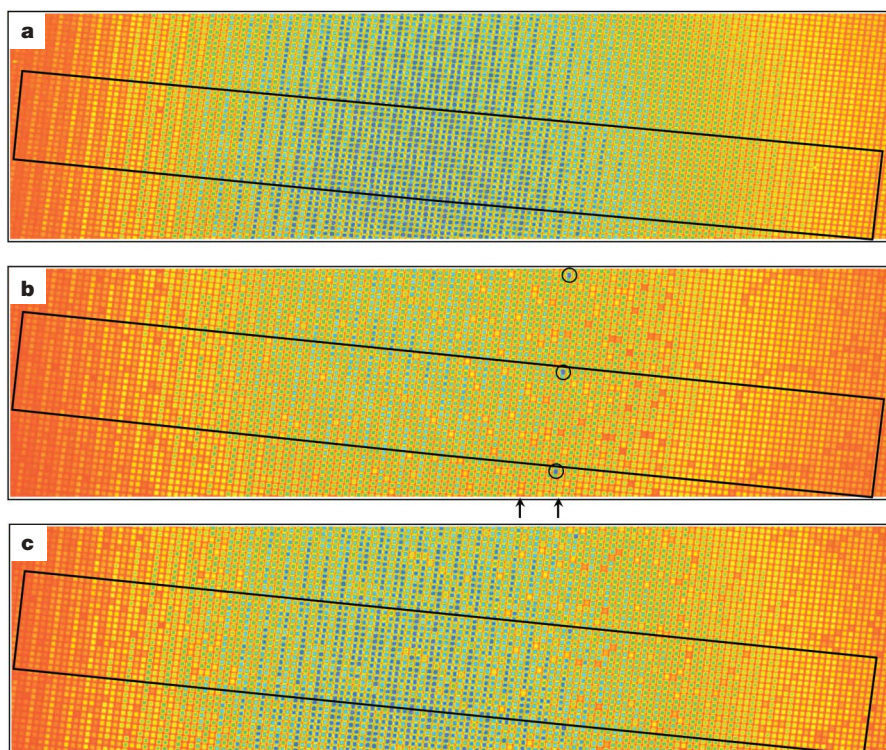


**Figure 2 | Two-dimensional spectrograms of optical frequency 'brush'.** The array of 'dots' is the false-colour image of  $\sim 2,200$  individual modes spanning 6.5 THz. (For the chosen colour map, blue represents higher optical power; a standard dilation filter was applied to aid visual clarity, and this causes the individual modes to have a square-like appearance.) In the vertical direction of this image, the data repeat every 50 GHz, and a subset of unique data are enclosed by the black box superimposed on the data. **a**, Background image taken without iodine present. **b**, Image acquired with iodine present. Numerous modes are attenuated owing to absorption by the iodine vapour, thus providing a unique fingerprint of the molecular vapour. The circled modes are those of a reference laser used in the calibration of the data. **c**, Same as **b** but with a different value of  $f_{\text{rep}}$  for the frequency comb, revealing a different set of absorbing transitions.

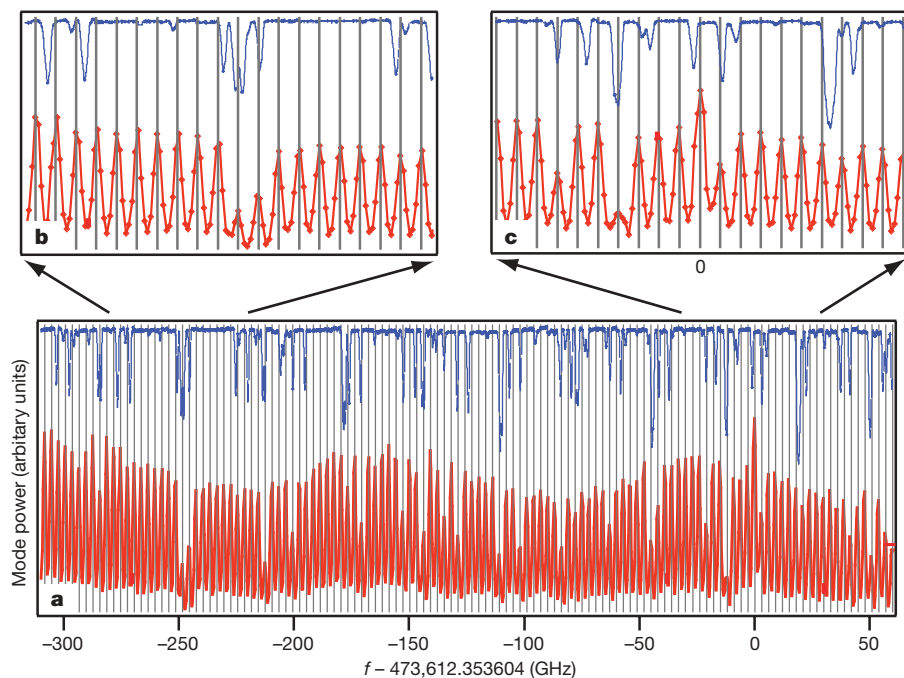


**Figure 3 | Concatenated line spectra.** **a**, Adjacent line spectra from seven columns identified by arrows in Fig. 2b are concatenated to show the power detected from >100 individual modes (red traces, bottom axis). No dilation filtering was applied in this case. Modes that are attenuated owing to the absorption of the iodine vapour appear with smaller amplitude relative to adjacent modes. The slow (~150 GHz) amplitude modulation arises from imperfections in the imaging and is of no physical consequence. Vertical grey lines identify the calculated mode frequencies, while the blue trace along the upper axis is the measured transmission spectra of iodine using CW laser techniques<sup>20</sup>. **b, c**, Expanded sections from **a** showing the attenuation of specific modes, the 1.2 GHz resolution limit of the spectrometer, and the pixelization of the CCD camera (small points on the red trace).

coincidence with various absorbing transitions in the iodine. At room temperature, the Doppler-broadened linewidth of the iodine transitions is ~400 MHz; however, the hyperfine splitting causes additional broadening of the lines to ~1–2 GHz.

An advantage of using the self-referenced frequency-stabilized comb for this spectroscopy is that the frequencies of the modes emitted from the laser are absolutely fixed according to  $\nu_n = n f_{\text{rep}} + f_0$ , where  $n$  is the integer mode index ( $n \approx 500,000$ ). In principle, each pixel of the CCD image then can be assigned a unique frequency. However, this requires that  $n$  be determined for each of the imaged modes, keeping in mind that only one-third of the original modes are transmitted by the filter cavity. In this example, the calibration is accomplished with the aid of a continuous wave (CW) He–Ne

laser stabilized to the well-known  $a_{16}$  component (line ‘f’) of the R(127)11–5 transition in  $^{127}\text{I}_2$ , with frequency equal to 474,612.353604 GHz (ref. 19). This laser is overlapped with the frequency comb in a single-mode optical fibre, and sent through the same high-resolution spectrometer. Its output is visible in Fig. 2b as the three noticeably more intense modes (corresponding to three orders of the VIPA) that are circled. Simultaneous heterodyne measurement between the He–Ne laser and the filtered frequency comb in a separate high-speed detector yields unique identification of the mode index  $n$  and absolute frequency calibration. Following the labelling technique shown diagrammatically in Fig. 1c, adjacent columns consisting of 16 modes can then be concatenated to display the data on a more traditional linear frequency axis. This is done for the

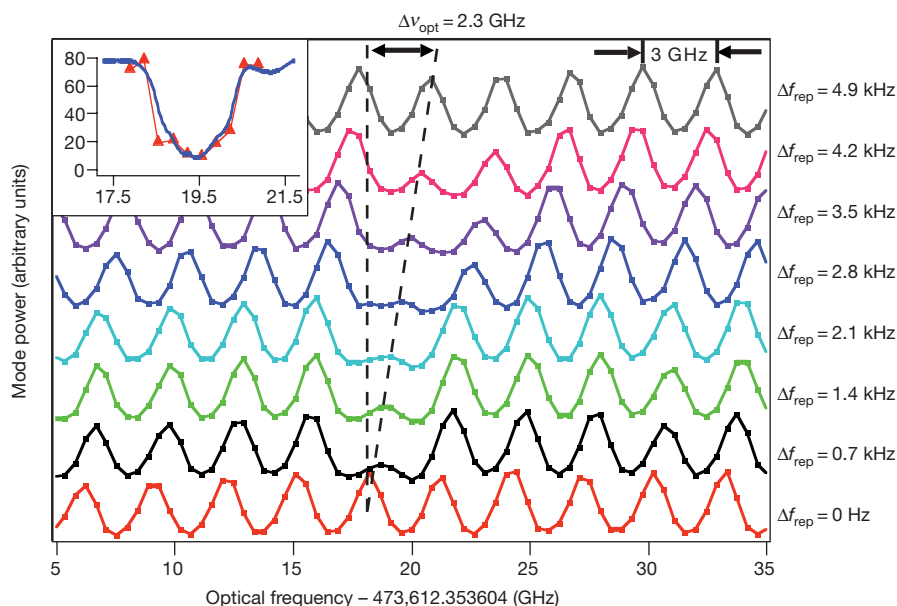


**Figure 4 | Absorption spectra of P(32)6–3, R(59)8–4 and R(53)8–4 transitions in iodine.** Eight line spectra, each obtained from images similar to Fig. 2, are offset vertically for clarity. In the successive spectra, the repetition rate ( $f_{\text{rep}}$ ) was increased by 700 Hz. As a result, a specific optical mode is scanned a total of  $\Delta\nu_{\text{opt}} = 2.3$  GHz with ~330 MHz steps across the absorption feature due to the overlapping P(32)6–3, R(59)8–4 and R(53)8–4

transitions<sup>22</sup>. The inset shows the de-convolved absorption feature (red triangles representing the relative transmission through the iodine versus the same optical frequency of the abscissa of the main plot), obtained from a fit to the peak value of the attenuated mode. The result of CW laser spectroscopy (blue line)<sup>20</sup> is shown for comparison.

seven columns between the arrows at the bottom of Fig. 2b, and the result is given in Fig. 3. The lower trace (red) in each of the plots of Fig. 3 is obtained from concatenating line traces along the unprocessed CCD image. Along the top axis, we also plot (blue) the iodine transmission spectra obtained from CW laser spectroscopy<sup>20</sup>. The calculated positions of the comb modes are indicated by the vertical (grey) lines. Only modes that coincide with an iodine transition are attenuated, thus demonstrating the potential for this technique to yield quantitative and accurate results.

The width of the intensity peaks in Fig. 3 data show the spectrometer resolution to be  $\sim 1.2$  GHz at 474 THz, which is within a factor of two of the calculated resolution. This is well-matched to the pixel resolution of the camera, which corresponds to about 440 MHz. However, this should not be confused with the linewidth of the comb modes, which is  $\sim 100$  kHz with the present maser reference, but could be significantly smaller ( $\sim 1$  Hz) with an optical reference for the frequency comb. Within the 1.2 GHz spectrometer resolution, we estimate that the absolute frequency position of an individual comb element is determined to 20 kHz in 5 ms of averaging, decreasing to 100 Hz at 1 s. Scanning the repetition rate of the laser (with the filter cavity also tracking) enables one to scan out the full optical spectrum with a resolution suitable for the system under study. In Fig. 2c a second image of the same spectral region but with a different repetition rate is shown. Visual differences with Fig. 2b are clearly seen. More quantitative results are obtained by again comparing line traces from images acquired with different repetition rates. This is shown in Fig. 4, where line traces covering 30 GHz are displayed for eight different values of  $f_{\text{rep}}$  offset sequentially by 700 Hz—corresponding to a 330 MHz offset from trace-to-trace in the optical domain. In this manner, a specific absorption feature can be mapped. Rapid electronic tuning of the repetition rate under computer control would yield a complete scan over many THz with appropriate resolution ( $\sim 200$  MHz) for Doppler-limited spectroscopy at video rates.

Although the straightforward absorption spectroscopy performed here is sufficient for strong transitions, the high resolution of this approach would benefit from cavity-enhanced sensitivity (achieved by, for example, putting the vapour cell inside an optical cavity), as has been demonstrated in the case of broadband cavity ring-down spectroscopy<sup>21</sup>. Additionally, multiple spectrometers at various wavelengths could be combined with image correlation techniques for identification of species of interest. In fact, the ability to spatially isolate and detect the individual modes of the stabilized frequency comb will give a way to implement (in a massively parallel manner) almost any of the powerful CW laser spectroscopic techniques that have been developed.

Received 23 September; accepted 12 December 2006.

1. Udem, T., Holzwarth, R. & Hansch, T. W. Optical frequency metrology. *Nature* **416**, 233–237 (2002).
2. Diddams, S. A. *et al.* An optical clock based on a single trapped  $^{199}\text{Hg}^+$  ion. *Science* **293**, 825–828 (2001).

3. Baltuska, A. *et al.* Attosecond control of electronic processes by intense light fields. *Nature* **421**, 611–615 (2003).
4. Bartels, A., Oates, C. W., Hollberg, L. & Diddams, S. A. Stabilization of femtosecond laser frequency combs with subhertz residual linewidths. *Opt. Lett.* **29**, 1081–1083 (2004).
5. Oskay, W. H. *et al.* Single-atom optical clock with high accuracy. *Phys. Rev. Lett.* **97**, 020801 (2006).
6. Marian, A., Stowe, M. C., Lawall, J. R., Felinto, D. & Ye, J. United time-frequency spectroscopy for dynamics and global structure. *Science* **306**, 2063–2068 (2004).
7. Gerginov, V., Tanner, C. E., Diddams, S. A., Bartels, A. & Hollberg, L. High-resolution spectroscopy with a femtosecond laser frequency comb. *Opt. Lett.* **30**, 1734–1736 (2005).
8. Shirasaki, M. Large angular dispersion by a virtually imaged phased array and its application to a wavelength demultiplexer. *Opt. Lett.* **21**, 366–368 (1996).
9. Xiao, S. & Weiner, A. M. 2-D wavelength demultiplexer with potential for  $\geq 1000$  channels in the C-band. *Opt. Express* **12**, 2895–2901 (2004).
10. Jiang, Z., Seo, D. S., Leaird, D. E. & Weiner, A. M. Spectral line-by-line pulse shaping. *Opt. Lett.* **30**, 1557–1559 (2005).
11. Baklanov, Y. V. & Chebotayev, V. P. Narrow resonances of two-photon absorption of super-narrow pulses in a gas. *Appl. Phys.* **12**, 97–99 (1977).
12. Teets, R., Eckstein, J. & Hänsch, T. W. Coherent two-photon excitation by multiple light pulses. *Phys. Rev. Lett.* **38**, 760–764 (1977).
13. Jones, D. J. *et al.* Carrier-envelope phase control of femtosecond mode-locked lasers and direct optical frequency synthesis. *Science* **288**, 635–639 (2000).
14. Lepetit, L., Cheriaux, G. & Joffe, M. Linear techniques of phase measurement by femtosecond spectral interferometry for applications in spectroscopy. *J. Opt. Soc. Am. B* **12**, 2467–2474 (1995).
15. Bartels, A. & Kurz, H. Generation of a broadband continuum by a Ti:sapphire femtosecond oscillator with a 1-GHz repetition rate. *Opt. Lett.* **27**, 1839–1841 (2002).
16. Ramond, T. M., Diddams, S. A., Hollberg, L. & Bartels, A. Phase-coherent link from optical to microwave frequencies by means of the broadband continuum from a 1-GHz Ti:sapphire femtosecond oscillator. *Opt. Lett.* **27**, 1842–1844 (2002).
17. Wang, S. X., Xiao, S. & Weiner, A. M. Broadband, high spectral resolution 2-D wavelength-parallel polarimeter for dense WDM systems. *Opt. Express* **13**, 9374–9380 (2005).
18. Jenkins, F. A. & White, H. E. *Fundamentals of Optics* 4th edn (McGraw Hill, New York, 1976).
19. Quinn, T. J. Practical realization of the definition of the metre, including recommended radiations of other optical frequency standards (2001). *Metrologia* **40**, 103–133 (2003).
20. Kato, H. *Doppler-Free High Resolution Spectral Atlas of Iodine Molecule 15000 to 19000 cm<sup>-1</sup>* (Japan Society for the Promotion of Science, Tokyo, 2000).
21. Thorpe, M. J., Moll, K. D., Jones, R. J., Safdi, B. & Ye, J. Broadband cavity ringdown spectroscopy for sensitive and rapid molecular detection. *Science* **311**, 1595–1599 (2006).
22. Simonsen, H. R. & Rose, F. Absolute measurements of the hyperfine splittings of six molecular  $^{127}\text{I}_2$  around the He-Ne/ $\text{I}_2$  wavelength at  $\lambda \approx 633$  nm. *Metrologia* **37**, 651–658 (2000).

**Acknowledgements** We thank A. M. Weiner for discussions about the VIPA spectrometer, and J. Ye for discussions that motivated our application of frequency combs to broadband spectroscopy. We further thank J. Stalnaker and Y. LeCoq for their comments on this manuscript, and H. Kato for the CW iodine spectroscopy data. This paper is a contribution of the National Institute of Standards and Technology, with partial support from DARPA.

**Author Information** Reprints and permissions information is available at [www.nature.com/reprints](http://www.nature.com/reprints). The authors declare no competing financial interests. Correspondence and requests for materials should be addressed to S.A.D. ([sdiddams@boulder.nist.gov](mailto:sdiddams@boulder.nist.gov)).